Characteristics of an Extreme Rainfall Event in Kyushu District, Southwestern Japan in Early July 2020

Yasutaka Hirockawa[1], Teruyuki Kato[2], Kentaro Araki[1], and Wataru Mashiko[1]
[1]*Meteorological Research Institute, Tsukuba, Japan*
[2]*Meteorological College, Kashiwa, Japan*

Abstract

An extreme rainfall event brought precipitation amounts exceeding 1000 mm in Kyushu district, southwestern Japan, in early July 2020. Especially, an elongated and stagnated mesoscale convective system formed around the Kuma River in central Kyushu district produced localized heavy rainfall with precipitation amounts larger than 600 mm in 13 hours. Characteristics of this extreme rainfall event were investigated using distributions of radar/raingauge-analyzed precipitation amounts (RAP) and statistically compared with those during the warm seasons (April–November) in 2009−2019. The results are shown as follows; (1) nine heavy rainfall areas of linear-stationary type (LS-HRAs) were extracted, (2) spatial and temporal scales of two LS-HRAs among them respectively exceeded 270 km and 10 hours, (3) the maximum RAP exceeding 100 mm in LS-HRAs were comparable to those in previous extreme rainfall events, (4) large accumulated three-hour precipitation amounts exceeding 200 mm were more frequently observed than those in the previous events, and (5) the accumulated five-day precipitation amount integrated around Kyushu Island was the largest since 2009. This study also showed that the large area-integrated precipitation amount was produced mainly from widespread precipitation systems associated with the Baiu front, while the nine LS-HRAs significantly contributed localized heavy rainfall.

(**Citation**: Hirockawa, Y., T. Kato, K. Araki, and W. Mashiko, 2020: Characteristics of an extreme rainfall event in Kyushu district, southwestern Japan in early July 2020. *SOLA*, **16**, 265−270, doi:10.2151/sola.2020-044.)

1. Introduction

Extreme rainfall events have often occurred in Kyushu district, southwestern Japan (Fig. 1a) during the Baiu season when rainy and moisture weather has been observed frequently from June and July (e.g., Ninomiya 1978; Ninomiya and Akiyama 1974, 1992; Ishihara et al. 1994; Ogura et al. 1985; Nagata and Ogura 1991; Kato 1998, 2006; Moteki et al. 2004), and their temporal and spatial scales and precipitation amounts were varied by each case. For instance, heavy rainfall areas (HRAs) widespread in an extreme rainfall event on 5−8 July 2018, which brought accumulated 24-hour precipitation amounts exceeding 500 mm (Tsuguti et al. 2019; Takemi and Unuma 2019; Tsuji et al. 2020; Yokoyama et al. 2020). On the other hand, HRAs concentrated in a narrow region in an extreme rainfall event on 5 July 2017, and most of the rainfall was produced by stagnated mesoscale convective systems (MCSs) (Kato et al. 2018; Kawano and Kawamura 2020). Quasi-stationary MCSs have often occurred around the Baiu front and brought localized heavy rainfall to Kyushu district, and frequently had a band-shaped structure (e.g., Ogura et al. 1985; Nagata and Ogura 1985; Kato 1998, 2005; Yoshizaki et al. 2000). Such the elongated and stagnated type of MCSs (ES-MCSs) is named "senjo-kousuitai" in Japanese (Kato 2020) and is recently noticed as a significant factor of extreme rainfall events.

Characteristics of ES-MCSs observed in Japan have been statistically investigated. Tsuguti and Kato (2014) demonstrated that approximately 60% of extreme rainfall events, not directly related to tropical cyclones, were caused by band-shaped precipitation systems, especially approximately 90% in Kyushu district. Unuma and Takemi (2016) showed that elongated MCSs were dominant during the warm season and mostly oriented in a southwest-northeast direction that was related to a shear direction at low levels (1000−700 hPa). Hirockawa et al (2020, hereafter HK20) proposed a procedure for the objective identification and classification of HRAs into four types (e.g., linear-stationary, linear, stationary, and others). HK20 also indicated that almost the same characteristics of HRAs with the linear-stationary type were found in those of the above-mentioned two studies, e.g., most of HRAs corresponded to typical ES-MCSs suggested in previous studies.

An extreme rainfall event with precipitation amounts over 1000 mm occurred in Kyushu district on 3−8 July 2020 (Fig. 2b), and hereafter it is abbreviated as "ER20 event". Many destructive floods, debris flows, and landslides were caused by heavy rainfall in ER20 event, which led to over 70 deaths, especially large rainfall amounts around the Kuma River (Fig. 2a) caused serious disasters. Heavy rainfall in ER20 event that occurred around the Baiu front (Fig. 1a) were caused by not only widespread precipitation associated with synoptic weather systems but also many ES-MCSs with hourly precipitation amounts exceeding 100 mm (Araki et al. 2021). It was a rare case that ES-MCSs caused heavy rainfall were observed concentratedly during several days. The examination on such characteristics of ES-MCSs in ER20 event is necessary for the understanding of EC-MCS structures and formation mechanisms.

The purpose of this study is to clarify the characteristics of HRAs and their contribution to total rainfall amounts in ER20 event. We objectively extract and classify HRAs in ER20 event by the procedure developed by HK20, and then examine the characteristics of HRAs by focusing especially the linear-stationary type. Moreover, the characteristics in temporal and spatial scales and intensities of the HRAs are compared with those of HRAs in extreme rainfall events during the past 11 warm seasons (April–November in 2009−2019). Furthermore, the characteristics are also statistically compared by classifying synoptic fields according to HK20.

2. Data and methods

Radar/raingauge-analyzed precipitation amounts (RAP, Nagata 2011), which are the hourly accumulated precipitation amounts with a resolution of 1 km (0.0125° × 0.00833°) produced by the Japan Meteorological Agency (JMA) and are converted with a resolution of 5 km (0.0625° × 0.05°) by the method of HK20, are used to investigate the characteristics of rainfall distributions. Accumulated three-hour RAP (RAP3), produced with one-hour intervals, are used to identify HRAs.

Although the procedure of HK20 could extract approximately 80% of HRAs with the linear-stationary type (LS-HRAs), typical LS-HRAs sometimes failed to be extracted. Therefore, HRAs are extracted and classified by the procedure of HK20 modified as follows; (1) four connected-component labeling is used instead of eight connected-component labeling for the identification of HRA

Corresponding author: Yasutaka Hirockawa, Meteorological Research Institute, 1-1 Nagamine, Tsukuba, Ibaraki 305-0052, Japan. E-mail: yhirockawa@mri-jma.go.jp.

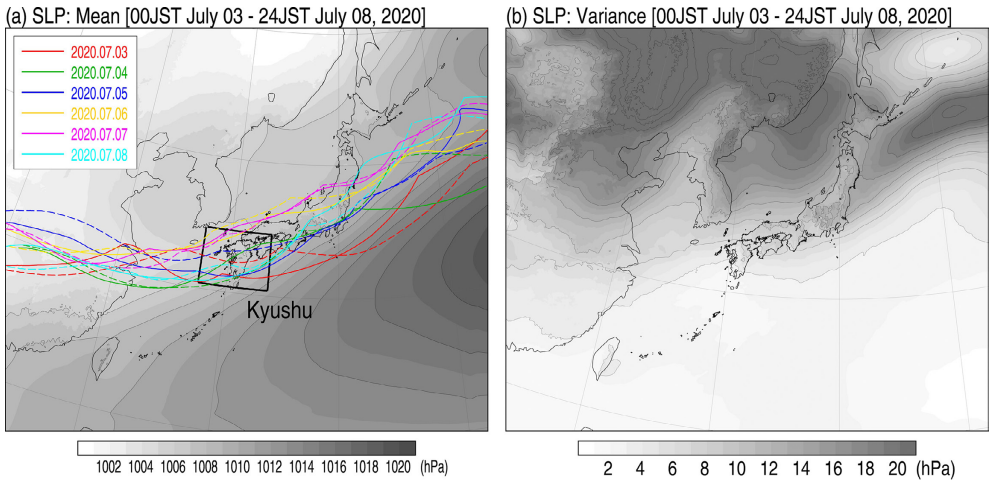

Fig. 1. (a) Mean and (b) variance fields of sea level pressure (shading and contour) derived from three hourly available JMA meso-scale objective analyses between 3−8 July 2020. The contours in (a) and (b) are drawn at 2 hPa and 3 hPa intervals, respectively. Colored curves in (a) (indicate the locations of the Baiu front between 3−8 July and solid and dashed lines imply 09 JST and 21 JST, respectively.

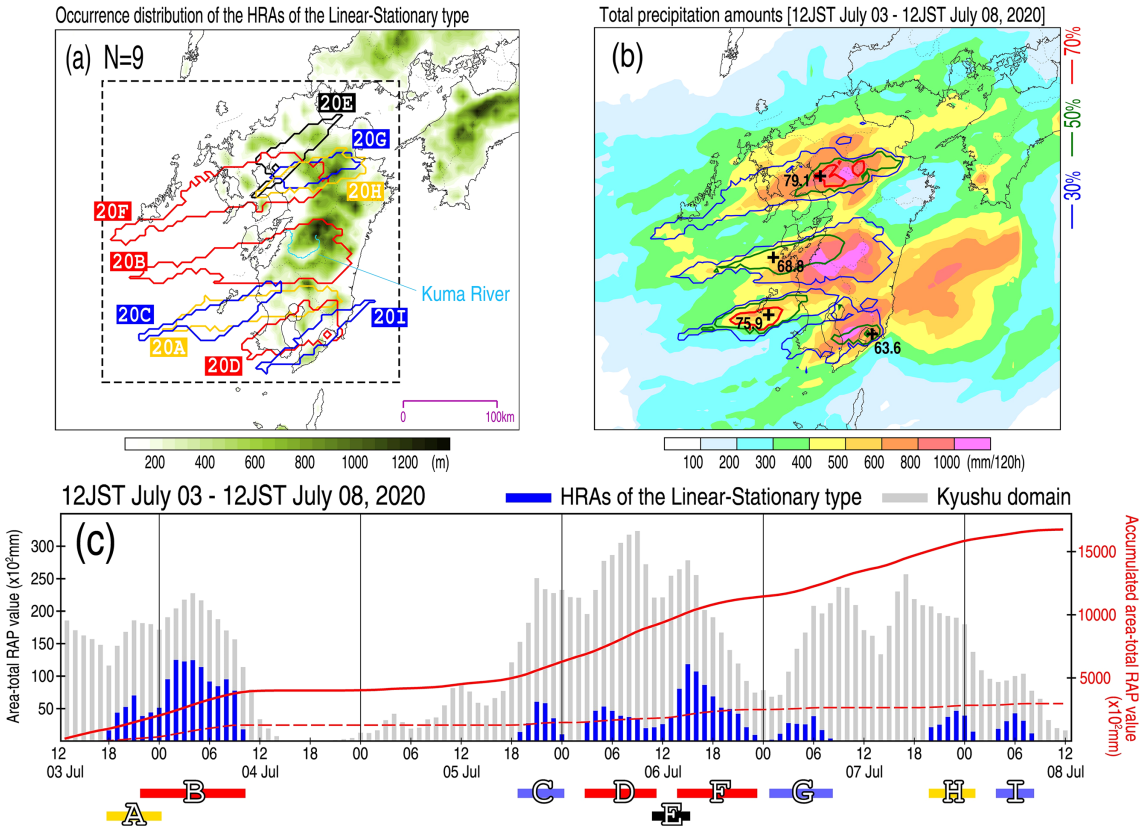

Fig. 2 (a) Occurrence distributions of LS-HRAs (contour) and topography (m, shading), and (b) their contribution ratio (%, contour) to the total precipitation amounts (mm, shading) (CRH) between 12 JST 3 July and 12 JST 8 July 2020. The dashed rectangle in (a) indicates the Kyushu domain used in this study. The blue, green, and red lines in (b) represent CRHs of 30, 50, and 70%, respectively. Crosses and labels in (b) imply the locations and the maximum values for each CRH closed curve. (c) Temporal variations of hourly area-total RAP of LS-HRAs (blue bars) and the Kyushu domain (gray bars), and integrated area-total RAP (red lines; dashed: LS-HRAs, solid: the Kyushu domain). Horizontal bars in (c) represent the occurrence periods for the LS-HRAs labeled in (a), but omitting "20".

candidates, (2) the criterion of an overlap ratio to aggregate HRAs is reduced to 40% from 50%, (3) the criterion of HRA areas are identified from each configuration before the aggregation, and (4) HRAs are classified as the linear-stationary type (LS-HRA) when aspect ratios of one or more HRA candidates that compose an aggregated HRA satisfy a criterion of 2.5. The modified procedure from HK20 can extract more appropriately LS-HRAs, i.e., the number of HRA extracts (400) increased about two times more than that (188) extracted by the original procedure during the warm seasons (April–November) in 2009−2019 (Fig. S1 in Supplement). Consequently, the LS-HRAs corresponded better than that extracted by the original procedure for matching typical EC-MCSs suggested in previous studies (e.g., Table 2 in Kato 2020).

For convenience, the following two kind variables are defined;

(1) "total RAP" that means a precipitation amount accumulated for arbitrary hours on a fixed grid, and (2) "area-total RAP" that means an integrated precipitation amount of total RAP for an area of each HRA or the Kyushu domain (denoted as dashed rectangle in Fig. 2a; 128.125°E−132.125°E, 30.9°N−34.1°N).

Synoptic fields are classified according to HK20, based on surface weather maps with six-hour intervals produced by JMA.

3. Results

Firstly, synoptic environment conditions that caused heavy rainfall are clarified. Figure 1a shows the sea level pressure field averaged using three-hour available JMA meso-scale objective analysis (Honda et al. 2005) between 3−8 July 2020, and the locations of the Baiu front subjectively detected at 09 JST (= UTC + 9 hours) and 21 JST every day. The Baiu front slightly oscillates within a few hundred kilometers in a meridional direction around Kyushu district. The synoptic field in ER20 event is categorized according to HK20 as stationary front (SF). Pacific subtropical high expands southwestward and almost stagnated with small variances of sea level pressure (Fig. 1b). Low-level warm and moist air flowed to Kyushu district along the edge of this Pacific subtropical high (Araki et al. 2021).

3.1 Characteristics of LS-HRAs

Nine LS-HRAs are extracted, which is the highest the number of the appearance for five days since 2009, and total precipitation amounts exceeding 1000 mm are distributed around the LS-HRAs between 12 JST 3 July and 12 JST 8 July 2020 (Figs. 2a and 2b). Corresponding to the meridional oscillation of the Baiu front, the LS-HRAs appear in difference areas in Kyushu district (Fig. 2a) that are located on the southern side of the Baiu front. Four LS-HRAs (20A, 20B, 20C, and 20F) extend from the sea far west of Kyushu Island to inland, and the horizontal scales of 20B and 20F exceed 270 km. The 20B correspond to LS-HRAs which caused severe damages around the Kuma River. On the other hand, the horizontal scales of LS-HRAs (20D, 20E, 20G, and 20H) that form mainly in an inland area are less than 150 km. Araki et al. (2021) indicated that stagnated MCSs formed along a low-level convergence line/zone on the sea associated with Baiu frontal depressions (Ninomiya 1978; Tochimoto and Kawano 2017). This low-level convergence on the sea might contribute to differences of the horizontal scale of LS-HRAs.

The contribution ratios of precipitation amounts associated with LS-HRAs to total precipitation (CRH), which are proposed by HK20, are distributed around 40% and the maximum value is approximately 80% around northern Kyushu district, i.e. for overlapping area on 20E, 20F, 20G, and 20H (Fig. 2b). The CRH for 20B is approximately 70% which is the maximum value from a single LS-HRA (Fig. 2b). Furthermore, the CRH for 20B in a shorter period (e.g., between 12 JST July 3 and 12 JST July 4) exceeds 70% in almost the whole area and has the maximum value of 94% (Fig. S2 in Supplement). These indicate that LS-HRAs strongly contribute to localized heavy rainfall, but not so large to the total precipitation in ER20 event.

The time series of area-total RAP for each LS-HRAs and the Kyushu domain are also examined (Fig. 2c). Two largest LS-HRAs (20B and 20F) that persist for more than 10 hours have area-total RAP exceeding 0.8×10^5 mm, which resulted in large CRHs (Figs. 2b and S2 in Supplement). The integrated area-total RAP for all LS-HRAs is approximately 20% of that for the Kyushu domain. These results ascertain that the CRH is small for the Kyushu domain while LS-HRAs significantly contribute to localized heavy rainfall.

The characteristics of LS-HRAs in ER20 event are compared with those of 134 LS-HRAs that are extracted in Kyushu district during the past 11 warm seasons in 2009−2019 (past LS-HRAs). The past LS-HRAs are frequently observed on the western and southern sides of Kyushu district and are oriented in various directions (Figs. 3a and 3b). In the synoptic field with a stationary front (SF), which is categorized when a distance between the location with the maximum rainfall amount in LS-HRAs and SF is within 500 km, the dominant orientation of past LS-HRAs is a south-west-northeast or west-east direction, and the two orientations appear with a comparable frequency except for the eastern coastal side of Kyushu Island (Figs. 3c and 3d). The past LS-HRAs for SF (60 cases) appeared more frequently than those for the other synoptic fields, and approximately 80% of them appeared associated with the Baiu front (not shown). The past LS-HRAs that orients in a south-north direction often appear associated with tropical cyclones (Fig. S3 in Supplement). The dominant orientation of LS-HRAs and synoptic field in ER20 event correspond well to those of the past LS-HRAs for SF, but some LS-HRAs (20B, 20C, and 20F in Fig. 2a) extend from the sea far west of Kyushu Island to inland, which is not found for past LS-HRAs for SF.

The characteristics of rainfall amounts associated with LS-HRAs are examined by comparing those of past LS-HRAs. This comparison is focused on past LS-HRAs that are observed around the Baiu front in typical extreme rainfall events, which are shown in Fig. 3d (09A and 09B in July 2009; 12A and 12B in July 2012; 17A in July 2017). Figure 4 depicts the relationships between horizontal scales and rainfall amounts of LS-HRAs, which is not clearly found between synoptic fields with SF and the other synoptic fields. The horizontal scales exceeding 270 km for 20B and 20F are the largest, and the persistent period of 13 hours for 20B is also the longest since 2009 (not shown). In ER20 event, the maximum RAP reaches approximately 100 mm for six LS-HRAs, but approximately 60 mm for two LS-HRAs (Fig. 4a). The maximum RAP3 exceeding 280 mm for 20B is comparable to those for 09B and 12A, although it is smaller than that for 17A (Fig. 4b). The maximum total RAP for 20B is approximately 650 mm and slightly smaller than that for 17A, but larger than those of the other past LS-HRAs (Fig. 4c). The area-total RAP for 20B (~1.1×10^5 mm) is larger than that for past LS-HRAs because the spatial and temporal scales are larger than the others (Table 1). It should be noted that the LS-HRAs in ER20 event have various rainfall amounts, e.g., the amounts for 20B are much larger than those for 20E and 20I. Analyses of environmental conditions in which each LS-HRA formed are our future issues.

Positive correlations (0.41−0.44) are found in the relation between the horizontal scales and rainfall amounts of past LS-HRAs. This relation exhibits clearer in RAP3 of LS-HRAs in ER20 event (positive correlation of 0.61). It should be noted that 17A has significant rainfall amounts despite of the horizontal scale less than 70 km. HK20 suggested that the stagnation of MCSs could increase not only total RAP but also the maximum RAP3. The relationship between rainfall amounts and spatial and temporal scales of LS-HRAs should be examined, which remains in our future works.

3.2 Characteristics of the appearance frequencies of large RAP

To additionally examine the characteristics of rainfall amounts in ER20 event, appearance frequencies of large RAP are compared with those for HRAs during the past 11 warm seasons. Figures 5a and 5b show the appearance frequencies of the number of 5 km grids with RAP exceeding 100 mm and RAP3 exceeding 200 mm in the Kyushu domain, judged every hour when HRAs are extracted, respectively. Higher numbers of the grids frequently appear associated with LS-HRAs. These results indicate that LS-HRAs often cause localized heavy rainfall. In ER20 event, the highest number of the grids with RAP exceeding 100 mm is 10 at 21 JST 3 July 2020, which is not particularly large (Fig. 5a). On the other hand, the highest number of the grids with RAP3 exceeding 200 mm is 36 at 03 JST 4 July 2020, which is the highest record since 2009 (Fig. 5b). All of the grids with RAP3 exceeding 200 mm in ER20 event are associated with four LS-HRAs (20B, 20C, 20D, and 20F), and they are the most frequently observed associated with 20B. Such frequent observations of large RAP3 is a remarkable feature in ER20 event, which might be a significant factor causing severe floods and landslides around the Kuma River.

Figure 5c shows the appearance frequencies of classified area-total RAP for the Kyushu domain for five days that is

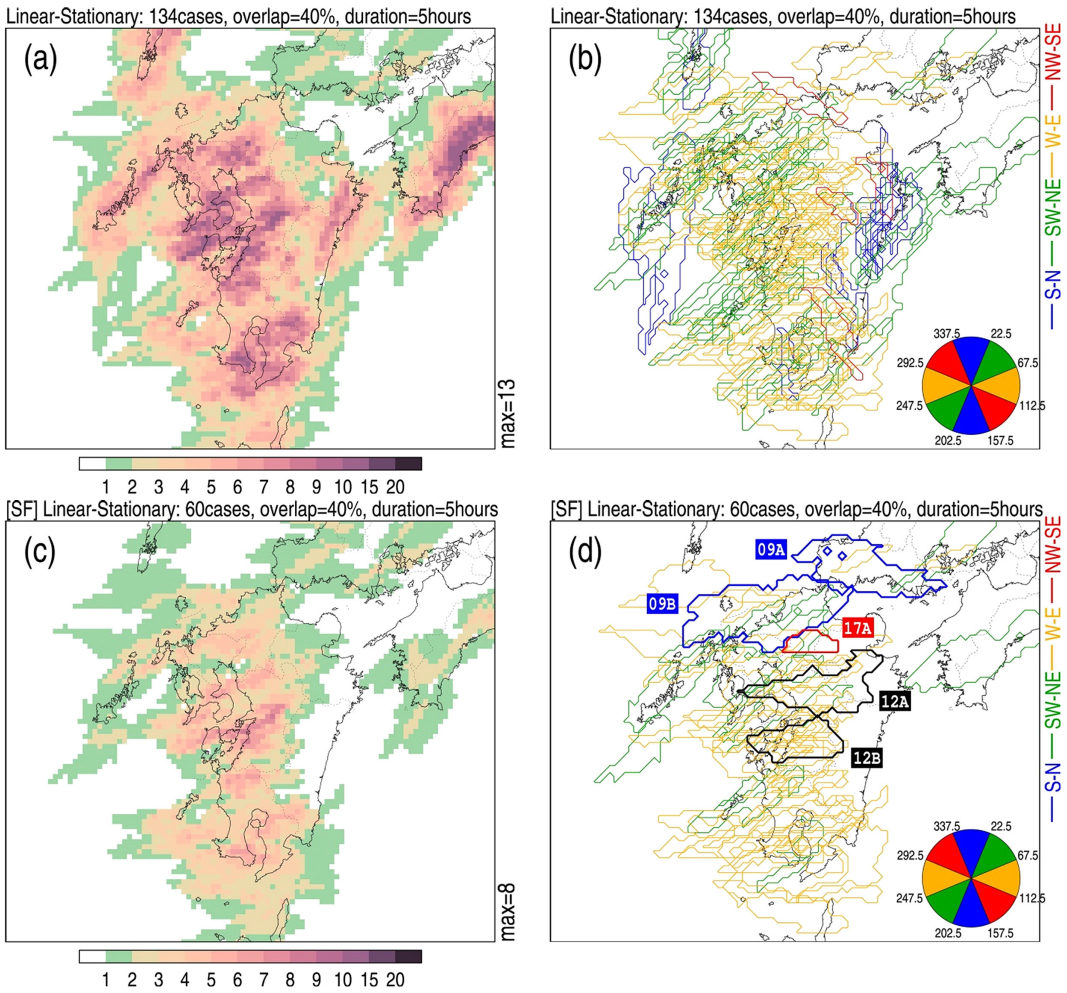

Fig. 3. Distributions of (a) the geographical appearance frequencies of the past LS-HRAs and (b) their orientations for all synoptic fields. (c, d) Same as (a, b), but for those with a stationary front. The closed curves in (b, d) show the LS-HRAs boundaries, and their colors indicate their orientations; the blue, green, yellow, and red colors represent the south-north, southwest-northeast, west-east, and northwest-southeast orientations, respectively. Bold solid curves in (d) denote LS-HRAs occurred in the past extreme rainfall events.

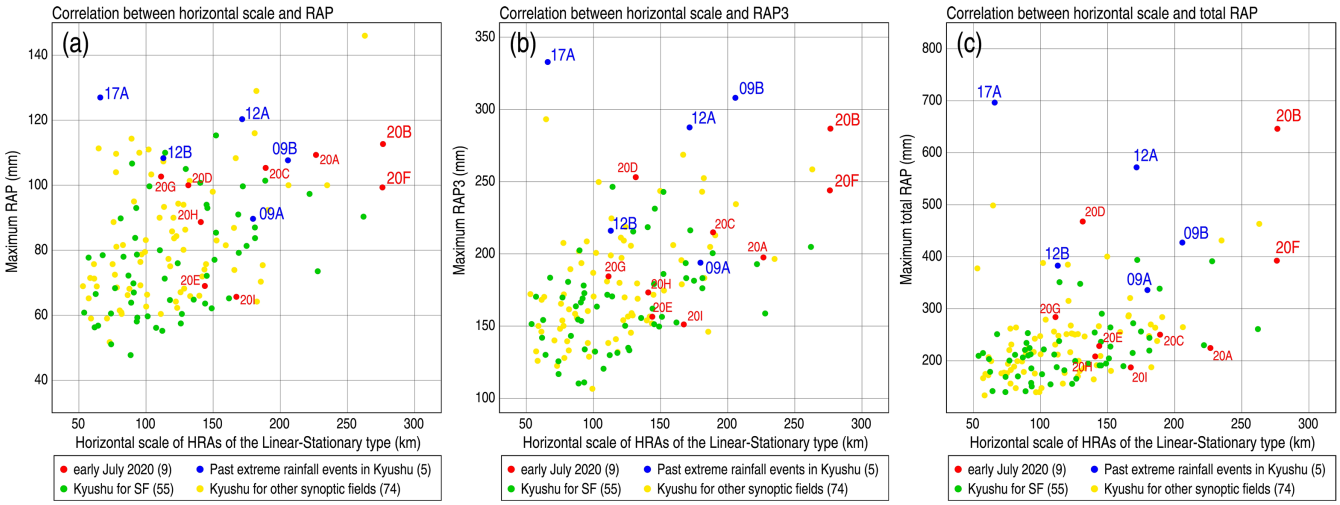

Fig. 4. Scatter diagrams of (a) the maximum RAP, (b) the maximum RAP3, and (c) total RAP of LS-HRAs (mm, ordinate) for their horizontal scales (km, abscissa). Closed red and blue circles with a label indicate LS-HRAs in ER20 event and the past extreme rainfall events, respectively; closed green and yellow circles denote the past LS-HRAs for SF and the other synoptic fields in Kyushu district, respectively.

Table 1. Characteristics of typical LS-HRAs occurred in ER20 event (20B) and the past extreme rainfall events (17A, 12A, and 09B) in Kyushu district.

	20B	17A	12A	09B
period (hours)	21 JST 3 July – 10 JST 4 July 2020 (13 hours)	12 JST 5 July – 22 JST 5 July 2017 (10 hours)	23 JST 11 July – 09 JST 12 July 2012 (10 hours)	14 JST 24 July – 22 JST 24 July 2009 (8 hours)
length (km)	277	66	172	206
max/mean RAP (mm)	112.7/27.9	127.0/40.3	120.3/30.8	107.7/30.0
max/mean RAP3 (mm)	286.7/80.0	332.8/107.7	287.5/84.0	308.0/78.5
max/mean toal RAP (mm)	646.0/300.5	696.5/322.6	571.9/246.3	427.3/210.0
area-total RAP (mm)	106374	14839	47296	72231

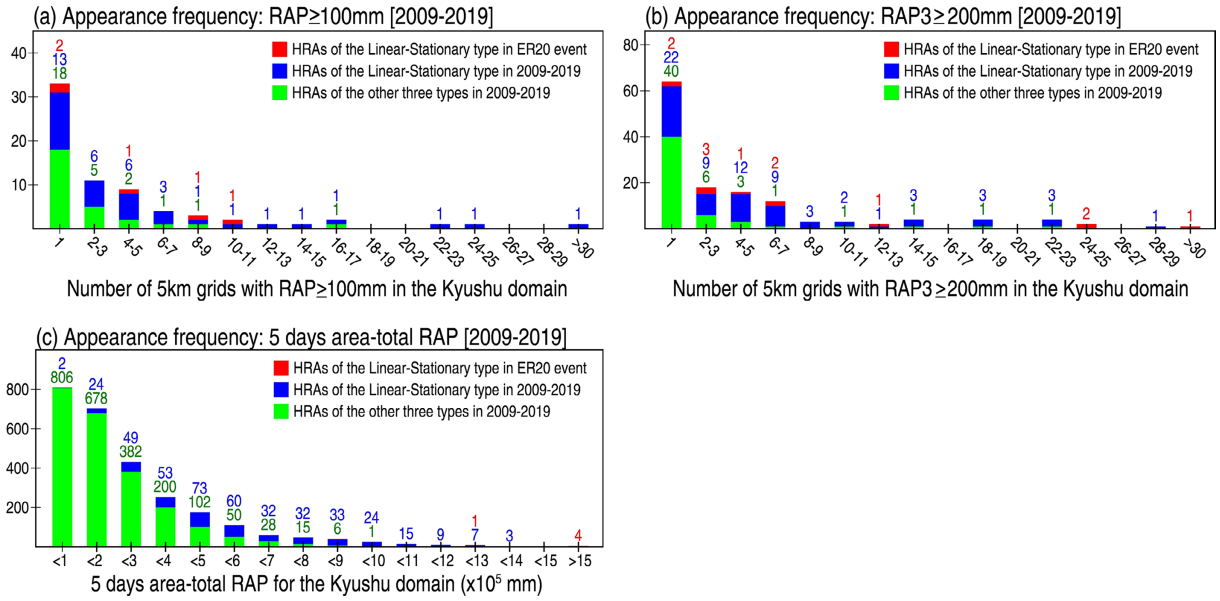

Fig 5. Appearance frequencies of the number of 5 km grids with (a) RAP exceeding 100 mm and (b) RAP3 exceeding 200 mm in the Kyushu domain during the warm seasons (April–November) in 2009−2019 and the ER20 event. (c) Same as (a) and (b), but for classified area-total RAP for the Kyushu domain for five days, which is represented by the daily maximum. The Red and blue bars respectively denote the number related to LS-HRAs in ER20 event and past LS-HRAs, whereas the green bars represent the number related to the other types of HRAs. The numbers above each bar denote the appearance frequencies of each category.

represented by the daily maximum. Huge amounts exceeding 10.0×10^5 mm are found limitedly when LS-HRAs are observed. The largest area-total RAP exceeding 16.8×10^5 mm is observed between 12 JST 3 July and 12 JST 8 July 2020 in ER20 event. Although such large precipitation amounts were brought mainly from widespread precipitation systems associated with the Baiu front, approximately 20% of them was contributed by LS-HRAs (Fig. 2c), which sometimes caused localized heavy rainfall with precipitation amounts exceeding 100 mm h^{-1} and/or 200 mm $(3h)^{-1}$ (Fig. 4).

4. Summary

An extreme rainfall events with precipitation amounts exceeding 1000 mm occurred in Kyushu district in early July 2020. The characteristics of this heavy rainfall were investigated using RAP and statistically compared with those of extreme rainfall events during the warm seasons (April–November) in 2009−2019 in Kyushu district. The characteristics of ER20 event obtained in this study are summarized in the following. Nine LS-HRAs were extracted, which is the highest number of the appearances for five days since 2009. The spatial and temporal scale of two LS-HRAs among them respectively reached 270 km and 10 hours, especially the persistent period of 13 hours for 20B is the longest since 2009. The maximum RAP, RAP3, and total RAP of LS-HRAs exceeded 100 mm, 200 mm and 600 mm, respectively; especially large RAP and RAP3 were observed in a LS-HRA (20B in Fig. 2a) detected around the Kuma River and the total-area RAP for 20B was significantly larger than those associated with past LS-HRAs. Number of 5 km grids with RAP3 exceeding 200 mm was more frequently observed than that in the previous events. Area-total RAP for the Kyushu domain reached 16.8×10^5 mm for five days, which was also the largest since 2009. Huge precipitation amounts in ER20 event were produced mainly from widespread precipitation systems associated with the Baiu front, while the nine LS-HRAs contributed localized heavy rainfall.

In this study the characteristics of heavy rainfall were investigated and examined using RAP; however, the formation and development processes and favorable occurrence conditions of ES-MCSs causing LS-HRAs remain unrevealed. These issues should be solved by performing objective analyses and numerical simulations as our future works.

Acknowledgements

The authors are grateful to two anonymous reviewers and the editor Prof. C. C. Wang for providing useful comments. Radar/raingauge-analyzed precipitation products, weather maps, and mesoscale objective analysis from the JMA were used in this study.

Edited by: C.-C. Wang

Supplements

Figure S1: Distributions of the geographical appearance frequencies of LS-HRAs and their configurations extracted by the modified and original procedures of HK20.

Figure S2: Contribution ratios of the LS-HRAs to the total precipitation amounts between 12 JST 3 July and 12 JST 4 July 2020.

Figure S3: Distributions of the geographical appearance frequencies and their orientations of LS-HRAs classified for synoptic fields.

References

Araki, K., T. Kato, Y. Hirockawa, and W. Mashiko, 2021: Characteristics of atmospheric environments of quasi-stationary convective bands in Kyushu, Japan during the July 2020 heavy rainfall event. *SOLA*, **17**, doi:10.2151/sola.2021-002.

Hirockawa, Y., T. Kato, H. Tsuguti, and N. Seino, 2020: Identification and classification of heavy rainfall areas and their characteristic features in Japan. *J. Meteor. Soc. Japan*, **98**, 835−857.

Honda, Y., M. Nishijima, K. Koizumi, Y. Ohta, K. Tamiya, T. Kawabata, and T. Tsuyuki, 2005: A pre-operational variational data assimilation system for a non-hydrostatic model at the Japan Meteorological Agency: Formulation and preliminary results. *Quart. J. Roy. Meteor. Soc.*, **131**, 3465−3475.

Ishihara, M., Y. Fujiyoshi, A. Tabata, H. Sakakibara, K. Akaeda, and H. Okamura, 1994: Dual doppler radar analysis of intense mesoscale rainband generated along the Baiu front in 1988: Its kinematical structure and maintenance process. *J. Meteor. Soc. Japan*, **73**, 139−163.

Kato, R., K. Shimose, and S. Shimizu, 2018: Predictability of precipitation caused by linear precipitation systems during the July 2017 Northern Kyushu heavy rainfall event using a cloud-resolving numerical weather prediction model. *J. Disas. Res.*, **13**, 846−859.

Kato, T., 1998: Numerical simulation of the band-shaped torrential rain observed over southern Kyushu, Japan on 1 August 1993. *J. Meteor. Soc. Japan*, **76**, 97−128.

Kato, T., 2005: Statistical study of band-shaped rainfall systems, the Koshikijima and Nagasaki lines, observed around Kyushu Island, Japan. *J. Meteor. Soc. Japan*, **83**, 943−957.

Kato, T., 2006: Structure of the band-shaped precipitation system inducing the heavy rainfall observed over northern Kyushu, Japan on 29 June 1999. *J. Meteor. Soc. Japan*, **84**, 129−153.

Kato, T., 2020: Quasi-stationary band-shaped precipitation systems, named "senjo-kousuitai," causing localized heavy rainfall in Japan. *J. Meteor. Soc. Japan*, **98**, 485−509.

Kawano, T., and R. Kawamura, 2020: Genesis and maintenance processes of a quasi-stationary convective band that produced record-breaking precipitation in northern Kyushu, Japan on 5 July 2017. *J. Meteor. Soc. Japan*, **98**, 673−690.

Moteki, Q., H. Uyeda, T. Maesaka, T. Shinoda, M. Yoshizaki, and T. Kato, 2004: Structure and development of two rerged rainbands observed over the East China Sea during X–BAIU–99 Part I: meso-β-scale structure and development processes. *J. Meteor. Soc. Japan*, **82**, 19−44.

Nagata, K., 2011: Quantitative precipitation estimation and quantitative precipitation forecasting. *RSMC Tokyo Typhoon Center Technical Review*, No. 13, Japan Meteorological Agency, 37−50. (Available online at: https://www.jma.go.jp/jma/jma-eng/jma-center/rsmc-hp-pub-eg/techrev/text13-2.pdf, accessed 24 August 2020)

Nagata, M., and Y. Ogura, 1991: A modeling case study of interaction between heavy precipitation and a low-level jet over Japan in the Baiu season. *Mon. Wea. Rev.*, **119**, 1309−1336.

Ninomiya, K., 1978: Heavy rainfalls associated with frontal depression in Asian subtropical humid region (I) synoptic-scale features. *J. Meteor. Soc. Japan*, **56**, 253−266.

Ninomiya, K., and T. Akiyama, 1974: Band structure of mesoscale echo clusters associated with low-level jet stream. *J. Meteor. Soc. Japan*, **52**, 300−313.

Ninomiya, K., and T. Akiyama, 1992: Multi-scale features of Baiu, the summer monsoon over Japan and the East Asia. *J. Meteor. Soc. Japan*, **70**, 467−495.

Ogura, Y., T. Asai, and K. Dohi, 1985: A case study of a heavy precipitation event along the Baiu front in northern Kyushu, 23 July 1982: Nagasaki heavy rainfall. *J. Meteor. Soc. Japan*, **63**, 883−900.

Takemi, T., and T. Unuma, 2019: Diagnosing environmental properties of the July 2018 heavy rainfall event in Japan. *SOLA*, **15**, 60−65.

Tochimoto, E., and T. Kawano, 2017: Numerical investigation of development processes of Baiu frontal depressions Part I: Case studies. *J. Meteor. Soc. Japan*, **95**, 91−109.

Tsuguti, H., and T. Kato, 2014: Objective extraction of heavy rainfall events and statistical analysis on their characteristic features. *Tenki*, **61**, 455−469 (in Japanese).

Tsuguti, H., N. Seino, H. Kawase, Y. Imada, T. Nakaegawa, and I. Takayabu, 2019: Meteorological overview and mesoscale characteristics of the heavy rain event of July 2018 in Japan. *Landslides*, **16**, 363−371.

Tsuji, H., C. Yokoyama, and Y. N. Takayabu, 2020: Contrasting features of the July 2018 heavy rainfall event and the 2017 Northern Kyushu rainfall event in Japan. *J. Meteor. Soc. Japan*, **98**, 859−876.

Unuma, T., and T. Takemi, 2016: A role of environmental shear on the organization mode of quasi-stationary convective clusters during the warm season in Japan. *SOLA*, **12**, 111−115.

Yokoyama, C., H. Tsuji, and Y. N. Takayabu, 2020: The effects of an upper-tropical trough on heavy rainfall event in July 2018 over Japan. *J. Meteor. Soc. Japan*, **98**, 235−255.

Yoshizaki, M., T. Kato, Y. Tanaka, H. Takayama, Y. Shoji, H. Seko, K. Arao, K. Manabe, and members of X-BAIU-98 observation, 2000: Analytical and numerical study of the 26 June 1988 orographic rainband observed in western Kyushu, Japan. *J. Meteor. Soc. Japan*, **78**, 835−856.

Manuscript received 28 September 2020, *accepted 6 November 2020*
SOLA: *https://www.jstage.jst.go.jp/browse/sola/*